Journal of Nuclear Medicine, published on October 27, 2022 as doi:10.2967/jnumed.122.264725

Preclinical Evaluation of a Humanized Antibody Against Common Lymphatic Endothelial and Vascular Endothelial Receptor-1, ^{89}Zr- Desferrioxamine-Bexmarilimab, in a Rabbit Model of Renal Fibrosis

Olli Moisio[1], Jenni Virta[1], Emrah Yatkin[2,] Heidi Liljenbäck[1,3], Senthil Palani[1], Riikka Viitanen[1], Maxwell W.G. Miner[1], Vesa Oikonen[1], Tuula Tolvanen[4,5], Danielle J. Vugts[6], Pekka Taimen[7,8], Xiang-Guo Li[1,8,9], Maija Hollmén[8,10], Sirpa Jalkanen[8,10], Anne Roivainen[1,3,4,8]

[1]Turku PET Centre, University of Turku, Turku, Finland; [2]Central Animal Laboratory, University of Turku, Turku, Finland; [3]Turku Center for Disease Modeling, University of Turku, Turku, Finland; [4]Turku PET Centre, Turku University Hospital, Turku, Finland; [5]Department of Medical Physics, Turku University Hospital, Turku , Finland; [6]Department of Radiology and Nuclear Medicine, Amsterdam UMC, VU University, Amsterdam, The Netherlands; [7]Institute of Biomedicine, University of Turku and Department of Pathology, Turku University Hospital, Turku, Finland; [8]InFLAMES Research Flagship Center, University of Turku, Turku, Finland; [9]Department of Chemistry, University of Turku, Turku, Finland; [10]MediCity Research Laboratory, University of Turku, Turku, Finland.

Correspondence: Prof. Anne Roivainen, PhD, Turku PET Centre, Kiinamyllynkatu 4-8, FI-20520 Turku, Finland. Tel: +35823132862, Fax: +35822318191, E-mail: anne.roivainen@utu.fi

First author: Olli Moisio, PhD student, Turku PET Centre, Kiinamyllynkatu 4-8, FI-20520 Turku, Finland. Tel: +358400667067, Fax: +35822318191, E-mail: oamois@utu.fi

Word count: 4994; **Abstract word count:** 209

Running title: ^{89}Zr-DFO-bexmarilimab PET in rabbits

Conflict of interest: MH and SJ own stocks in Faron Pharmaceuticals. The remaining authors have no conflicts of interest to disclose.

Financial support: The study was financially supported by grants from Business Finland, the Jane and Aatos Erkko Foundation, and the Finnish Cultural Foundation. OM is a PhD student partially supported by the Drug Research Doctoral Programme of the University of Turku Graduate School and the doctoral module of the InFLAMES Flagship.

ABSTRACT

Bexmarilimab is a new humanized monoclonal antibody against common lymphatic endothelial and vascular endothelial receptor-1 (CLEVER-1), and is in clinical trials for macrophage-guided cancer immunotherapy. In addition to cancer, CLEVER-1 is also associated with fibrosis. To facilitate prospective human PET studies, we preclinically evaluated ^{89}Zr-labeled bexmarilimab in rabbits.

Methods: Bexmarilimab was conjugated with desferrioxamine (DFO) and radiolabeled with ^{89}Zr. Retained immunoreactivity was confirmed by flow cytometry. Distribution kinetics of intravenously administered ^{89}Zr-DFO-bexmarilimab (0.1 mg/kg) for up to 7 days in a rabbit model of renal fibrosis mediated by unilateral ureteric obstruction (UUO). The *in-vivo* stability of ^{89}Zr-DFO-bexmarilimab was evaluated by sodium dodecyl sulfate-polyacrylamide gel electrophoresis in combination with autoradiography. Additionally, we estimated the human radiation dose from data obtained in healthy rabbits.

Results: ^{89}Zr-DFO-bexmarilimab cleared rapidly from the blood circulation and distributed to the liver and spleen. At 24 hours post-injection, PET/CT, *ex-vivo* gamma counting and autoradiography demonstrated that there was significantly higher ^{89}Zr-DFO-bexmarilimab uptake in UUO-operated fibrotic renal cortex, characterized by abundant CLEVER-1-positive cells, than in contralateral or healthy kidneys. The estimated effective dose for a 70-kg human was 0.70 mSv/MBq.

Conclusion: The characteristics of ^{89}Zr-DFO-bexmarilimab support future human PET studies to, for example, stratify patients for bexmarilimab treatment, evaluate the efficacy of treatment, or monitor disease progression.

Key Words: bexmarilimab; CLEVER-1; PET/CT; renal fibrosis; whole-body distribution; zirconium-89

GRAPHICAL ABSTRACT

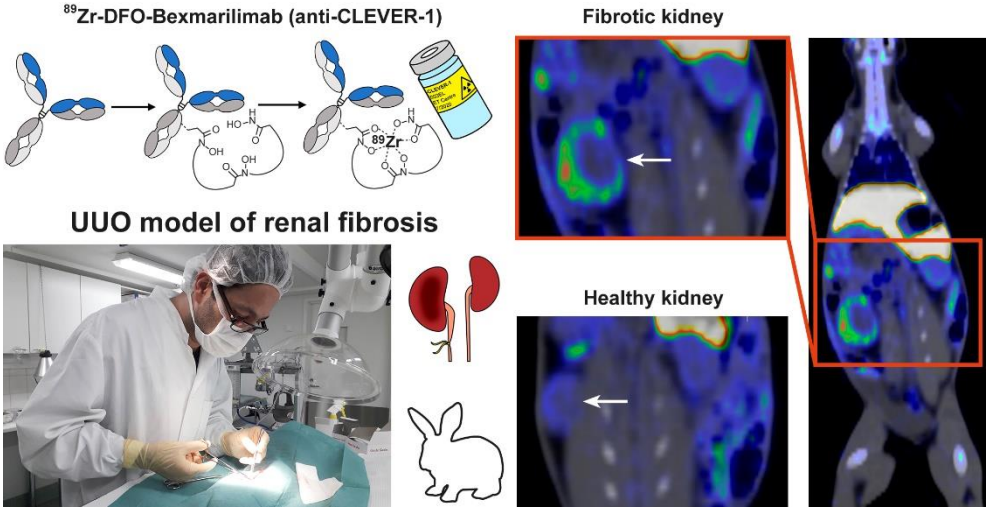

INTRODUCTION

Common lymphatic endothelial and vascular endothelial receptor-1 (CLEVER-1, also known as stabilin-1 and FEEL-1) is a multifunctional scavenger receptor expressed on anti-inflammatory, alternatively activated M2 macrophages (*1*,*2*). In addition, the molecule is present, as the name suggests, in the lymphatic and vascular endothelium. In human tissues, CLEVER-1 is specifically expressed in the non-continuous endothelial cells of the spleen, liver, adrenal cortex, and lymph nodes (*3*–*5*).

The humanized anti-CLEVER-1 antibody bexmarilimab (K_D 0.75×10^{9} M to human CLEVER-1) has been developed for immunotherapy, and has recently shown promising results in clinical trials (*6*). While the main research focus of studies investigating CLEVER-1 has been its effects on tumor-associated macrophages and cancer (*7*), CLEVER-1 mediates tissue homeostasis and prevents fibrosis in liver injury. In this context, CLEVER-1 protects against excessive fibrosis in response to oxidative stress by clearing modified low-density lipoproteins. The uptake of modified low-density lipoproteins reduces profibrogenic chemokine CCL3 secretion, resulting in reduced fibrosis and promotion of healing (*8*).

Therefore, we propose that CLEVER-1 may also be a relevant marker of tissue repair and the healing response in inflammatory diseases, and we present the preclinical evaluation of ^{89}Zr-labelled desferrioxamine (DFO)-conjugated bexmarilimab in a rabbit model of renal fibrosis. Notably, the parental anti-human CLEVER-1 antibody 3-372 can also recognize rabbit CLEVER-1 (*9*). To obtain a detailed assessment of the whole-body distribution kinetics of intravenously administered bexmarilimab and its CLEVER-1-targeting ability, we radiolabeled bexmarilimab and preclinically evaluated the effects of ^{89}Zr-DFO-bexmarilimab in healthy rabbits and rabbits with renal fibrosis induced by unilateral ureteral obstruction (UUO).

MATERIALS AND METHODS

Supplemental materials and methods are available at http://jnm.snmjournals.org).

Study Design

The study protocol is presented in Figure 1. The UUO model of renal fibrosis in rabbits was used as the animal model. Ligation of the left ureter was carried out in seven female New Zealand White rabbits 7 days prior to ^{89}Zr-DFO-bexmarilimab injection. Six healthy rabbits were studied as controls.

The whole-body distribution kinetics of intravenously (i.v.) administered ^{89}Zr-DFO-bexmarilimab were studied in rabbits (n=13, weight 2.12±0.19 kg) using *in-vivo* PET/CT imaging for up to 7 days, and *ex-vivo* gamma counting of excised tissues and digital autoradiography of kidney cryosections. Histology and immunohistochemistry supported the *ex-vivo* autoradiography. Renal perfusion was determined by ^{15}O-radiowater PET/CT prior to ^{89}Zr-DFO-bexmarilimab injection, and the kidney volume was determined by CT. Human radiation dose estimates for ^{89}Zr-DFO-bexmarilimab were extrapolated from healthy rabbit data.

All animal experiments were approved by the national Project Authorization Board in Finland (license numbers ESAVI/856/04.10.07/2017 and ESAVI/5882/2020), and were carried out in compliance with the EU Directive 2010/EU/63 on the protection of animals used for scientific purposes.

Preparation of ^{89}Zr-DFO-bexmarilimab

Bexmarilimab (IgG4, ~150 kDa, in 25 mg/mL stock solution containing 10 mM L-histidine/HCl pH 6.0, 20 mM L-methionine, 280 mM trehalose, and 0.02% polysorbate 20) was

obtained from Faron Pharmaceuticals, Turku, Finland (*10*). The desferrioxamine conjugation and radiolabeling of bexmarilimab with ^{89}Zr were carried out using a previously published protocol with slight modifications (*11*). To attach the hexadentate chelator desferrioxamine, bexmarilimab stock was reconstituted to a concentration of 3 mg/mL in sodium bicarbonate buffer (1.0 M, 1 mL, pH 9.0) by ultrafiltration (Amicon Ultra 60 kDa, Millipore). Subsequently, to 1 mL of the rebuffered antibody, isothiocyanatobenzyl-desferrioxamine (p-DFO-Bz-NCS, 10 µL, 3.5 mM in dimethyl sulfoxide [DMSO], 2 equivalents) was added and the solution was incubated at 37 °C for 30 minutes while mixing. Then, the reaction mixture was transferred onto a PD-10 size-exclusion column (Cytiva) and DFO-bexmarilimab was eluted in 1.5 mL formulation buffer containing 10 mM L-histidine, 20 mM methionine, 280 mM sucrose and 0.02% polysorbate 20 in water at pH 6.0 (adjusted with HCl).

The radiolabeling was performed by mixing 40–45 MBq of ^{89}Zr (Cyclotron VU; 100 µL, 1.0 M oxalic acid), Na_2CO_3 (45 µL, 2.0 M), HEPES buffer (500 µL, 0.5 M, pH 7.2) and DFO-bexmarilimab (355 µL, 1.3 mg/mL). The mixture was incubated at room temperature for 60 minutes while mixing. The crude product mixture was transferred onto a PD-10 size-exclusion column and ^{89}Zr-DFO-bexmarilimab was eluted in 1.5 mL of formulation buffer.

The radiochemical quality of ^{89}Zr-DFO-bexmarilimab was analyzed with two methods; ultrafiltration and sodium dodecyl sulfate-polyacrylamide gel electrophoresis (SDS-PAGE). For the ultrafiltration method, 5 µL of the product was added to a Microcon spin filter (60 kDa cut-off; Millipore) containing 95 µL 5% DMSO in phosphate-buffered saline. The product was centrifuged at 14,000×*g* for 6 minutes followed by two washes with 100 µL 5% DMSO in phosphate-buffered saline. The radioactivity remaining in the filter and filtrate was then separately measured with a γ-counter (Wizard 1480, PerkinElmer). The radiochemical purity of ^{89}Zr-DFO-

bexmarilimab was determined as the amount of radioactivity on the filter divided by the total amount of radioactivity multiplied by 100%. The measurements were performed in triplicate. SDS-PAGE was carried out to detect possible aggregates and larger fragments of antibodies. The assay was run on a Miniprotean electrophoresis system using pre-cast 4–20% non-denaturing Tris-glycine polyacrylamide gels (Bio-Rad). Subsequently, the gel was rinsed in water, placed on a phosphor imaging plate (Fujifilm), and after exposure scanned on a BAS-5000 scanner (Fujifilm). The resulting images were analyzed with AIDA image analyzer (Raytest) to determine the percentage of intact ^{89}Zr-DFO-bexmarilimab.

The immunoreactivity and CLEVER-1 binding of DFO-bexmarilimab and ^{89}Zr-DFO-bexmarilimab after radioactive decay were confirmed by flow cytometry using unmodified bexmarilimab (clone CP-12; Abzena) as a reference molecule. Briefly, peripheral blood mononuclear cells (Finnish Red Cross) enriched with CD14-microbeads (Miltenyi) or the CLEVER-1^{high} acute myelogenous leukemia cell line KG-1 (CCL-246; ATCC) were used. KG-1 cells were cultured in Iscove's modified Dulbecco's medium supplemented with 20% fetal bovine serum and penicillin/streptomycin. The cells (0.5×10^6 cells per well) were plated in a round-bottom 96-well plate (Sarstedt) and stained with varying concentrations (µg/mL) of bexmarilimab, DFO-bexmarilimab and ^{89}Zr-DFO-bexmarilimab. An irrelevent isotype IgG4 control antibody, (S241/L248E)-Alexa Fluor 647 (Abzena), was used to normalize the signal. The cells were stained with mouse anti-human IgG4-Alexa Fluor 488 (#9200-30; Southern Biotech). Fixed samples were subjected to flow cytometry on a LSRFortessa cell analyzer (Becton Dickinson) and analyzed with FlowJo10 (TreeStar Ashland) software.

Radiosynthesis of ^{15}O-Radiowater

^{15}O-radiowater was synthesized as previously described (*12*).

PET/CT Imaging

A Discovery-690 PET/CT (GE Medical Systems) device was used for imaging studies.

Rabbits were sedated and anesthetized with s.c. injection of a mixture of medetomidine (Cepetor Vet 1 mg/mL, CP-Pharma, 0.1 mg/kg) ketamine (Ketaminol 50 mg/kg, Intervet Oy, 2 mg/kg) and midazolam (Midazolam Hameln 5 mg/mL, Hameln, 0.1 mg/kg). For scanning on day 1, two cannulas were inserted, one in the left ear vein for injecting tracers and the other in the right ear vein or artery for blood sampling. For scans on day 2 onwards, only one ear vein was cannulated for blood sampling.

For measurement of renal perfusion, 20±0 MBq of ^{15}O-radiowater was injected i.v. and the rabbits were imaged for 6 minutes (frames 15×4 seconds, 4×10 seconds, 4×20 seconds, 3×60 seconds).

^{89}Zr-DFO-bexmarilimab (7.2±2.5 MBq [mean±SD], range 4.4–10.2 MBq, 3.5±1.3 MBq/kg, 0.1 mg/kg) was injected on the first scanning day, and dynamic whole-body PET/CT scanning was performed for 30 minutes immediately after the injection, then static whole-body scans were performed at 24 hours, 2 days, 3 days, and 7 days post-injection. Dynamic emission scans of 12 time frames (4×30 seconds, 4×60 seconds, 2×120 seconds, 2×600 seconds) were acquired by serial imaging of the body in two contiguous segments. Three bed positions were required for static whole-body PET, with a 6-minute acquisition time for each position.

PET/CT images were analyzed using Carimas software (www.turkupetcentre.fi/carimas/). Regions of interest were defined for the whole kidney (parenchyma), kidney cortex, kidney

medulla, heart left ventricle cavity (representing blood), liver, lungs, muscle, myocardium and spleen in the PET/CT images; the CT scan was used to provide an anatomical reference. The suprarenal abdominal aorta was used as the region of interest representing blood in ^{15}O-radiowater analyses. Kidney volumes were determined from CT images. Results are expressed as standardized uptake values (SUVs) and time–activity curves (TACs).

Renal perfusion was estimated by fitting a single-tissue compartmental model to the regional radioactivity concentration curves. An image-derived arterial blood curve was used as the model input function. The non-linear sum-of-least squares method was used to estimate perfusion ($mL_{blood}/mL_{tissue}\times min$) (*13*,*14*).

In-Vivo Stability of ^{89}Zr-DFO-Bexmarilimab

Blood samples (100–1,500 µL) were collected into heparinized tubes at 1 minute, 5 minutes, 10 minutes, 30 minutes, 1 hour, 2 hours, 3 hours, 4 hours, 24 hours, 2 days, 3 days, and 7 days after ^{89}Zr-DFO-bexmarilimab injection. The radioactivity of the whole blood samples was measured with a Wizard γ-counter (PerkinElmer). Plasma was subsequently separated by centrifugation (2,100×*g* for 5 minutes at 4°C) and radioactivity was measured using the γ-counter.

To determine the amount of intact ^{89}Zr-DFO-bexmarilimab, aliquots of plasma were applied to native SDS-PAGE as described above. Briefly, a small volume of plasma (up to 10 µL) was added to 10 µL of 4×Laemmli sample buffer (BioRad) and filled to a volume of 40 µL with H_2O and applied on the gel. For high radioactivity samples (0–4 hours post-injection), plasma was diluted with physiological saline prior to preparing the sample. ^{89}Zr-DFO-bexmarilimab in formulation buffer (stored at 4°C) was used as a reference.

Ex-Vivo Biodistribution and Digital Autoradiography

Rabbits were sacrificed either at 24 hours (UUO *n*=4, healthy *n*=3) or 7 days (UUO *n*=3, healthy *n*=3) after ^{89}Zr-DFO-bexmarilimab injection. After the last PET/CT imaging, the rabbits were sacrificed under deep ketamine-medetomidine-midazolam anesthesia by cardiac puncture and an overdose of pentobarbital (Mebunat, Orion Pharma). Tissues and organs were immediately dissected, weighed and assayed for radioactivity with a γ-counter (Wizard, PerkinElmer). The radioactive decay of ^{89}Zr ($T_{1/2}$=3.3 days) was corrected for the time of injection. The uptake of radioactivity is expressed as SUV.

Samples of kidneys were embedded and frozen in Tissue-Tek (Sakura), and cut into 8-µm and 20-µm slices. The 20-µm cryosections were thaw-mounted onto microscope slides and immediately exposed to a phosphor imaging plate (Fujifilm). After an exposure time of approximately 3 days, the imaging plates were scanned with a BAS-5000 scanner. After scanning, sections were stained with hematoxylin-eosin (H&E) and scanned with a digital slide scanner (Pannoramic 250 Flash, 3DHistec). The 8-µm sections were stored at −70°C and used for CLEVER-1 immunohistochemical staining as described below.

The accumulation of ^{89}Zr-DFO-bexmarilimab in the renal cortex and medulla was analyzed on superimposed autoradiographs and H&E images using Carimas software. Results were decay-corrected for injection and exposure time, normalized to the injected radioactivity dose, and expressed as the photostimulated luminescence per square millimeter (PSL/mm^2).

The 8-µm cryosections of kidneys and spleen were stained with anti-CLEVER-1 (clone 3-372, InVivo Biotech) peroxidase staining. Briefly, the slides were acetone fixed, blocked with horse serum and incubated overnight at 4°C in a humidified chamber with 10 µg/mL of clone 3-372 or mouse IgG1 control antibody. The signal was detected using a Vectastain Elite ABC kit

(Vector Laboratories) and liquid chromogen 3, 3'-diaminobenzidine substrate (DAKO). The slides were counterstained with hematoxylin and imaged with a Pannoramic digital slide scanner (3DHistec). Endogenous peroxidase activity was not blocked prior to staining because this procedure reduces the staining quality.

Additional formalin-fixed, paraffin-embedded 7-μm kidney sections were stained with Picrosirius red to evaluate kidney damage and the development of renal fibrosis.

Statistical Analysis

Results are expressed as the mean±SD. Differences between groups were determined with the independent samples t-test using Excel (Microsoft). *P* values of less than 0.05 were considered statistically significant.

RESULTS

Characterization of the UUO Rabbit Model

Visual and histological inspection of the left kidney demonstrated obvious damage (swollen, enlarged kidney) due to the blockage of urine flow to the bladder (Supplemental Fig. 1). The contralateral kidney appeared healthy with no obvious damage.

The renal perfusion parameters in rabbits 7 days after the UUO operation are presented in Figure 2A and Supplemental Table 1. The ^{15}O-radiowater PET analysis revealed that the renal perfusion was significantly lower in the UUO renal cortex (2.00±0.95 mL_{blood}/mL_{tissue}/min) than in the contralateral (5.57±1.96 mL_{blood}/mL_{tissue}/min, P=0.001) or healthy renal cortex (5.25±0.55 mL_{blood}/mL_{tissue}/min, P<0.001).

Based on *in-vivo* CT results, the volume of UUO-operated kidneys was enlarged, whereas the contralateral kidney was a similar size as the kidney from healthy rabbits (Fig. 2B).

The histopathological analysis showed dilation of renal tubules, focal injury of tubular epithelial cells and varying levels of inflammation in UUO kidneys. Additionally, Picrosirius red staining showed tubulointerstitial fibrosis of the renal cortex in UUO kidneys. There were no histological abnormalities in the contralateral kidney from UUO rabbits or kidneys from healthy control rabbits (Fig. 2C). Anti-CLEVER-1 staining of UUO kidneys showed specific immunoreactivity on recruited macrophages in the tubulointerstitium. The contralateral kidney or the kidney from healthy rabbits did not show this pattern of immunoreactivity (Fig. 2C). No significant differences in staining were observed between the 7- and 14-day samples.

Anti-CLEVER-1 staining of spleen and kidney sections, as well as H&E and Pictosirius red staining of kidney sections obtained 7 days and 14 days post-surgery are presented in Supplemental Figures 2 and 3.

Preparation of ^{89}Zr-DFO-Bexmarilimab and Immunoreactivity

The DFO-NCS conjugation and labeling method enabled us to obtain a final formulation of ^{89}Zr-DFO-bexmarilimab (Supplemental Fig. 4A) that was of excellent quality without antibody aggregates or fragments, as measured by SDS-PAGE. The retained immunoreactivity of DFO-bexmarilimab was 87.5%±2.2 (n=4) indicating that the modification with a chelator did not substantially alter antibody binding to CLEVER-1. Using four radiolabeled batches (n=4), we determined that ^{89}Zr-DFO-bexmarilimab had a radiochemical yield of 78.2%±4.2, specific radioactivity of 76.1±5.1 MBq/mg and a radioactivity concentration of 14.9±4.4 MBq/mL. The radiochemical purity was 99.1%±0.3 when measured by ultrafiltration and 100% when measured

by SDS-PAGE autoradiography (Supplemental Fig. 4B). When measured in a single batch, the immunoreactivity of ^{89}Zr-DFO-bexmarilimab after radioactive decay (approximately 4 weeks after radiolabeling, stored at –20°C) was similar to that of DFO-bexmarilimab (Supplemental Fig. 4C).

^{89}Zr-DFO-Bexmarilimab PET/CT Imaging and Biodistribution

In UUO and healthy rabbits, *in-vivo* PET/CT clearly visualized the liver and spleen, and showed that there was some uptake of ^{89}Zr-DFO-bexmarilimab in bone/bone marrow and intestines (Fig. 3A). The highest radioactivity concentration after i.v. injection of ^{89}Zr-DFO-bexmarilimab was seen in the liver but the concentration decreased over time (Supplemental Figs. 5 and 6). The radioactivity concentration was always higher in the renal cortex than in the medulla, and the UUO kidney cortex was clearly visualized (Fig. 3A).

The uptake of ^{89}Zr-DFO-bexmarilimab at 24 hours post-injection was significantly higher in the UUO renal cortex than in the contralateral or healthy renal cortex, and was even more pronounced when normalized to the level of renal perfusion (Figs. 3B and 3C). Decay-corrected TACs revealed that uptake of ^{89}Zr-DFO-bexmarilimab in the UUO renal cortex remained constant after 24 hours, but increased over time in the contralateral renal cortex (Fig. 3D).

Supplemental Table 2 shows the *ex-vivo* biodistribution of ^{89}Zr-DFO-bexmarilimab in rabbits at 24 hours and 7 days post-injection. The organs with the highest radioactivity concentration were the liver, spleen and bone/bone marrow; this result confirmed the *in-vivo* PET/CT findings. The lowest uptake was seen in the brain.

In-Vivo Stability and Plasma Pharmacokinetics of ^{89}Zr-DFO-Bexmarilimab

The SDS-PAGE analysis of serial plasma samples from UUO rabbits showed that the proportion of intact ^{89}Zr-DFO-bexmarilimab decreased from 97.0%±1.2 of total plasma radioactivity at 4 hours after tracer injection to 78.2%±13.1, 51.2%±9.8, and 33.2%±3.4 at 24 hours, 2 days, and 3 days, respectively. In healthy rabbits, the proportion of intact ^{89}Zr-DFO-bexmarilimab was 96.2%±0.1, 51.1%±8.5, 24.9%±6.6, and 15.6%±4.3, 4 hours, 24 hours, 2 days, and 3 days, respectively, after tracer injection (Figs. 4A and 4B). Representative autoradiographs of SDS-PAGE are shown in Supplemental Figure 7.

The blood-to-plasma ratio of radioactivity was about 0.6 and did not change appreciably over the 7-day PET study (Supplemental Fig. 8). The plasma pharmacokinetic parameters are summarized in Supplemental Table 3. ^{89}Zr-DFO-bexmarilimab had a relatively fast clearance from the blood circulation, with total clearance of 10.4±2.1 mL/h (n=3) in UUO rabbits and 17±2.1 mL/h (n=3) in healthy rabbits (P=0.030).

Digital Autoradiography

Digital autoradiography of rabbit kidney cryosections combined with H&E staining confirmed that ^{89}Zr-DFO-bexmarilimab was retained in the renal cortex (Fig. 5). Despite impaired renal perfusion in the UUO kidney, uptake 24 hours post-injection was higher in the UUO renal cortex and medulla than in the contralateral and healthy kidneys (P<0.05). At 7 days post-injection, the highest uptake was in the contralateral renal cortex; this finding is consistent with the results of PET/CT studies and *ex-vivo* gamma counting.

Radiation Dose Estimates

The human residence times (the normalized numbers of disintegrations) for the various source organs and the remainder of the body extrapolated from healthy rabbit data are listed in Supplemental Table 4. Supplemental Figure 9 shows the TACs of the organs on which the dosimetry calculation using OLINDA/EXM 2.1 was based. The estimates of the organ doses given in Supplemental Table 5 were calculated for a 70-kg adult male. The organs with the highest doses were the liver (5.860±1.100 mGy/MBq), gall bladder wall (2.580±0.420 mGy/MBq), and adrenal glands (1.777±0.240 mGy/MBq). The mean effective dose (ICRP 103; *14*) was calculated as 0.702±0.051 mSv/MBq. For example, a 37 MBq dose of ^{89}Zr-DFO-bexmarilimab would likely result in an effective dose of 26 mSv.

DISCUSSION

Bexmarilimab is a new humanized anti-CLEVER-1 antibody currently in clinical immunotherapy trials. In addition to its potential use as an immunotherapeutic, we are interested in determining whether the antibody is suitable for immuno-PET imaging. The information presented from this study increases our understanding of its pharmacokinetics and *in-vivo* biodistribution, and provides estimates for the human radiation dose, which will support future clinical translation of ^{89}Zr-DFO-bexmarilimab immuno-PET.

To enable ^{89}Zr-radiolabeling, bexmarilimab was successfully conjugated with a desferrioxamine chelator without compromising immunoreactivity, i.e., 87.5% of the immunoreactivity was retained. Subsequent radiolabeling resulted in the formation of ^{89}Zr-DFO-bexmarilimab that had a high radiochemical yield and high radiochemical purity. SDS-PAGE was a particularly suitable method to evaluate purity because it enabled all radioactive substances with

different molecular sizes, whether free ^{89}Zr or antibody aggregates, to be separated from the intact tracer in the same assay. Most importantly, conjugating bexmarilimab with ^{89}Zr and desferrioxamine did not lead to loss of immunoreactivity. This finding is important, since ^{89}Zr-DFO-bexmarilimab is intended for use in clinical PET applications.

CLEVER-1, as observed by anti-CLEVER-1 immunohistochemistry, was clearly expressed on macrophages residing in the UUO kidney, which were not present in the contralateral and healthy kidneys. PET/CT imaging, *ex-vivo* gamma counting and autoradiography analysis similarly showed significant differences in the uptake of ^{89}Zr-DFO-bexmarilimab into UUO kidneys compared with the contralateral and healthy kidneys at 24 hours post-injection. ^{89}Zr-DFO-bexmarilimab showed a surprisingly fast clearance coupled with fast initial uptake in the target tissues.

It should be noted that although the kidneys show uptake of ^{89}Zr-DFO-bexmarilimab at 24 hours post-injection, they are also a likely route of excretion of radiometabolites/fragments. We hypothesize that the increased uptake of tracer in the contralateral and healthy kidneys 7 days post-injection, as shown by PET/CT and *ex-vivo* results, is due to uptake of radiometabolites, given that the level of radiometabolites in the bloodstream increases in the days following the injection of ^{89}Zr-DFO-bexmarilimab. In UUO and healthy rabbits, radiometabolites consisted on average 84% and 67%, respectively, of the total plasma radioactivity on day 3 post-injection. Almost no intact ^{89}Zr-DFO-bexmarilimab was detected at day 7, although we note that the total plasma radioactivity at that time was too low for accurate detection. An approximate doubling of radioactivity uptake in the contralateral kidney compared with the healthy kidney at day 7 would support this hypothesis, as the contralateral kidney compensates for the loss of UUO kidney function. A likely

source of circulating metabolites may be the liver, as a decrease in liver radioactivity was observed after the 24 and 48 hour time points (Supplemental Fig. 6).

The fast uptake and clearance of ^{89}Zr-DFO-bexmarilimab highlight the importance of determining the optimal time window for PET studies to achieving meaningful results. In this study, the optimal time window is clearly at 24 hours, when tracer accumulation in the UUO kidney has stabilized, blood radioactivity has diminished and radiometabolites have not yet begun to accumulate in the healthy and contralateral kidneys.

In general, the uptake of ^{89}Zr-DFO-bexmarilimab in the liver and spleen corresponded to previously reported CLEVER-1 expression in human tissues (*3*–*5*). However, although we confirmed CLEVER-1 expression by immunohistochemical staining in the spleen and UUO kidneys, we did not analyze the liver and other tissues that possibly express CLEVER-1.

The estimated human radiation burden due to a single i.v. ^{89}Zr-DFO-bexmarilimab injection is comparable to that of other ^{89}Zr-labeled monoclonal antibodies (*14*–*16*), and is suitable for clinical studies. In this study, scaling between rabbit and human data was performed using organ and whole-body masses of rabbits and humans. Despite similarities between species, the accuracy of extrapolation of biokinetic data from laboratory animals to humans is uncertain, particularly for the liver due to qualitative differences between species in the handling of many elements by this organ.

CONCLUSION

Based on the preclinical results of this study, including the estimated human radiation burden, ^{89}Zr-DFO-bexmarilimab is suitable for future clinical PET studies.

DISCLOSURE

MH and SJ own stock in Faron Pharmaceuticals. The other authors declare that they have no conflicts of interest to disclose. The study was financially supported by Business Finland, the Jane and Aatos Erkko Foundation, and the Finnish Cultural Foundation. OM is a PhD student partially supported by the Drug Research Doctoral Program of the University of Turku Graduate School and the doctoral module of the InFLAMES Flagship.

ACKNOWLEDGMENTS

Timothy Johnson and Toby Holmes (Sheffield University, UK) are thanked for their advice and help regarding the UUO rabbit model. Professional assistance from Aake Honkaniemi (Turku PET Centre), Sari Mäki (MediCity Research Laboratory), Marja-Riitta Kajaala and Erika Nyman (the University of Turku Histocore Facility) is greatly appreciated. The personnel of the University of Turku Central Animal Laboratory are thanked for expert animal care. The authors thank Timo Kattelus for preparing the figures.

KEY POINTS

QUESTION: Are the characteristics of CLEVER-1-targeted ^{89}Zr-DFO-bexmarilimab suitable for prospective human PET studies?

PERTINENT FINDINGS: This preclinical rabbit study revealed that intravenously administered ^{89}Zr-DFO-bexmarilimab was able to detect fibrosis associated with abundant CLEVER-1-positive cells. The estimated human effective dose was within the safe limits for potential human use.

IMPLICATIONS FOR PATIENT CARE: Clinical studies to determine whether ^{89}Zr-DFO-bexmarilimab-PET is suitable for, for example, stratifying patients for bexmarilimab treatment, evaluating treatment efficacy, and monitoring disease progression, may be justified.

REFERENCES

1. Kzhyshkowska J, Gratchev A, Goerdt S. Stabilin-1, a homeostatic scavenger receptor with multiple functions. *J Cell Mol Med.* 2006;10:635–649.
2. Palani S, Maksimow M, Miiluniemi M, Auvinen K, Jalkanen S, Salmi M. Stabilin-1/CLEVER-1, a type 2 macrophage marker, is an adhesion and scavenging molecule on human placental macrophages. *Eur J Immunol.* 2011;41:2052–2063.
3. Goerdt S, Walsh LJ, Murphy GF, Pober JS. Identification of a novel high molecular weight protein preferentially expressed by sinusoidal endothelial cells in normal human tissues. *J Cell Biol.* 1991;113:1425–1437.
4. Hansen B, Longati P, Elvevold K, et al. Stabilin-1 and stabilin-2 are both directed into the early endocytic pathway in hepatic sinusoidal endothelium via interactions with clathrin/AP-2, independent of ligand binding. *Exp Cell Res*. 2005;303:160–173.
5. Martens JH, Kzhyshkowska J, Falkowski-Hansen M, et al. Differential expression of a gene signature for scavenger/lectin receptors by endothelial cells and macrophages in human lymph node sinuses, the primary sites of regional metastasis. *J Pathol*. 2006;208:574–589.
6. Virtakoivu R, Rannikko JH, Viitala M, et al. Systemic blockade of Clever-1 elicits lymphocyte activation alongside checkpoint molecule downregulation in patients with solid tumors: results from a phase I/II clinical trial. *Clin Cancer Res.* 2021;27:4205–4220.
7. Hollmén M, Figueiredo CR, Jalkanen, S. New tools to prevent cancer growth and spread: a 'CLEVER' approach. *Br J Cancer* 2020;123:501–509.
8. Rantakari P, Patten DA, Valtonen J, et al. Stabilin-1 expression defines a subset of macrophages that mediate tissue homeostasis and prevent fibrosis in chronic liver injury. *Proc Natl Acad Sci USA.* 2016;113:9298–9303.

9. Irjala H, Elima K, Johansson EL, et al. The same endothelial receptor controls lymphocyte traffic both in vascular and lymphatic vessels. *Eur J Immunol*. 2003;33:815–824

10. Hollmén M, Maksimow M, Rannikko JH, et al. Nonclinical characterization of bexmarilimab, a Clever-1-targeting antibody for supporting immune defense against cancers. *Mol Cancer Ther.* 2022;21:1207–1218.

11. Vosjan M, Perk L, Visser G. et al. Conjugation and radiolabeling of monoclonal antibodies with zirconium-89 for PET imaging using the bifunctional chelate p-isothiocyanatobenzyl-desferrioxamine. *Nat Protoc.* 2010;5:739–743.

12. Sipilä HT, Clark JC, Peltola O, Teräs M. An automatic [^{15}O]H2O production system for heart and brain studies. *J Label Compd Radiopharm*. 2001;44:S1066–S1068.

13. ICRP Publication 103: The 2007 recommendations of the international commission on radiological protection. *Ann ICRP*. 2007;37:1–333.

14. Börjesson PK, Jauw YW, de Bree R, et al. Radiation dosimetry of ^{89}Zr-labeled chimeric monoclonal antibody U36 as used for immuno-PET in head and neck cancer patients. *J Nucl Med.* 2009;50:1828–1836.

15. Laforest R, Lapi SE, Oyama R, et al. [^{89}Zr]Trastuzumab: evaluation of radiation dosimetry, safety, and optimal imaging parameters in women with HER2-positive breast cancer. *Mol Imaging Biol.* 2016;18:952–959.

16. O'Donoghue JA, Lewis JS, Pandit-Taskar N, et al. Pharmacokinetics, biodistribution, and radiation dosimetry for ^{89}Zr-trastuzumab in patients with esophagogastric cancer. *J Nucl Med.* 2018;59:161–166.

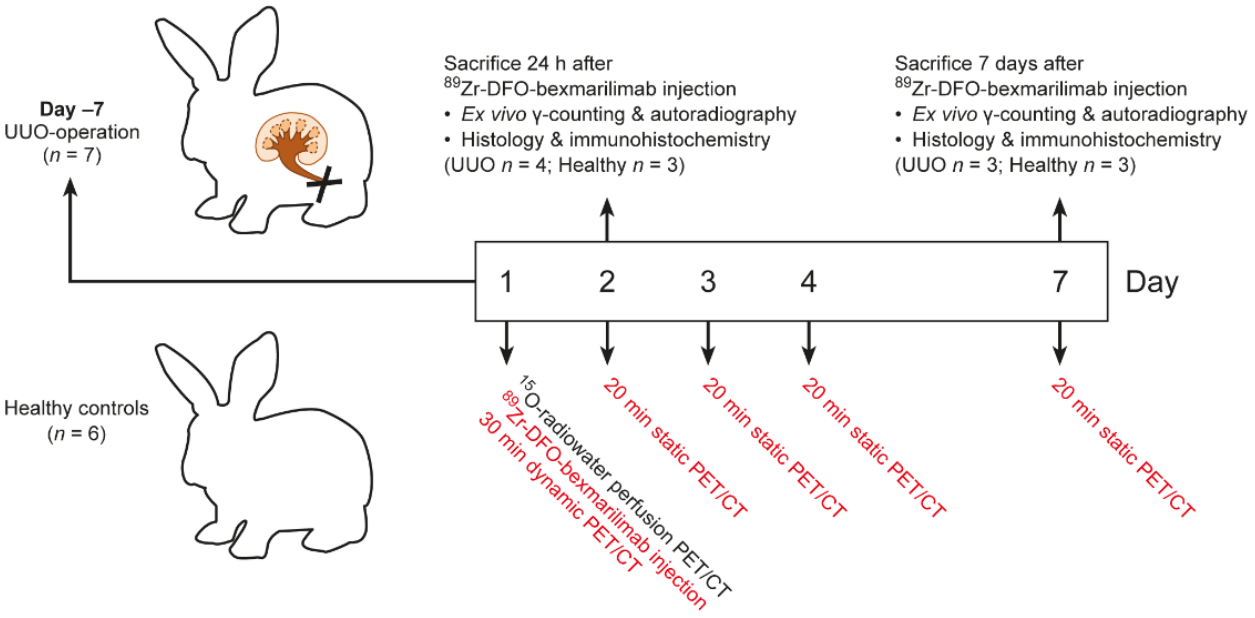

FIGURE 1. Study design. New Zealand White rabbits (*n*=6 healthy and *n*=7 unilateral ureteric obstruction (UUO); UUO surgery was performed 7 days before the start of the study, which began on day 1) were first examined for renal perfusion using ^{15}O-radiowater PET/CT, and then intravenously injected with ^{89}Zr-DFO-bexmarilimab for sequential PET/CT imaging for up to 7 days post-injection. Rabbits were sacrificed for post-mortem studies either 24 hours or 7 days after ^{89}Zr-DFO-bexmarilimab injection.

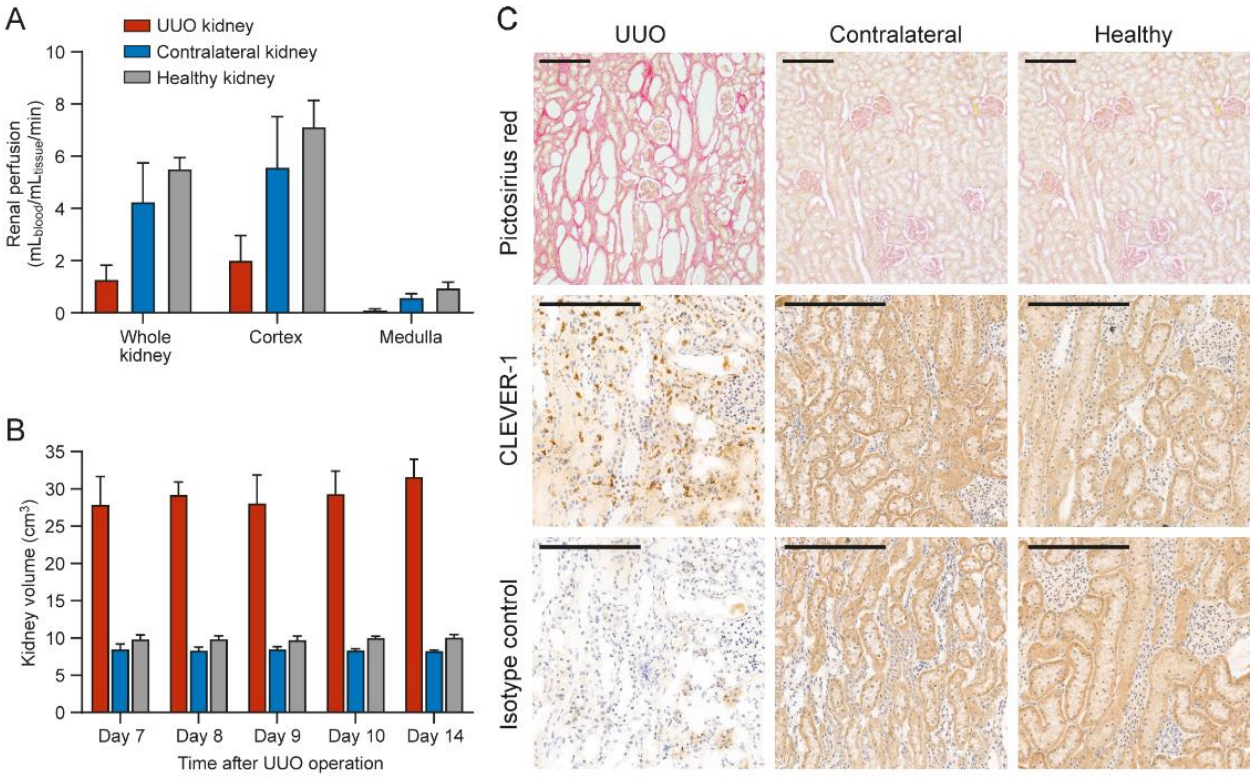

FIGURE 2. Characterization of the rabbit UUO model. (A) Renal perfusion determined using ^{15}O-radiowater PET/CT 7 days after the UUO operation. (UUO and contralateral *n*=6, healthy *n*=5) (B) Kidney volumes of UUO and healthy rabbits based on CT imaging (*n*=3). (C) Picrosirius red staining shows dilation of the renal tubules and tubulointerstitial fibrosis of the renal cortex in UUO kidneys while the histology is normal in the contralateral kidney from the same animal and in healthy control rabbits. Anti-CLEVER-1 immunohistochemical staining shows specific immunoreactivity in tissue macrophages in the UUO kidney. Light brown unspecific background staining from urine flow can be observed in the cortex area of contralateral and healthy kidney tissue but not in UUO tissue. The scale bar is 200 µm.

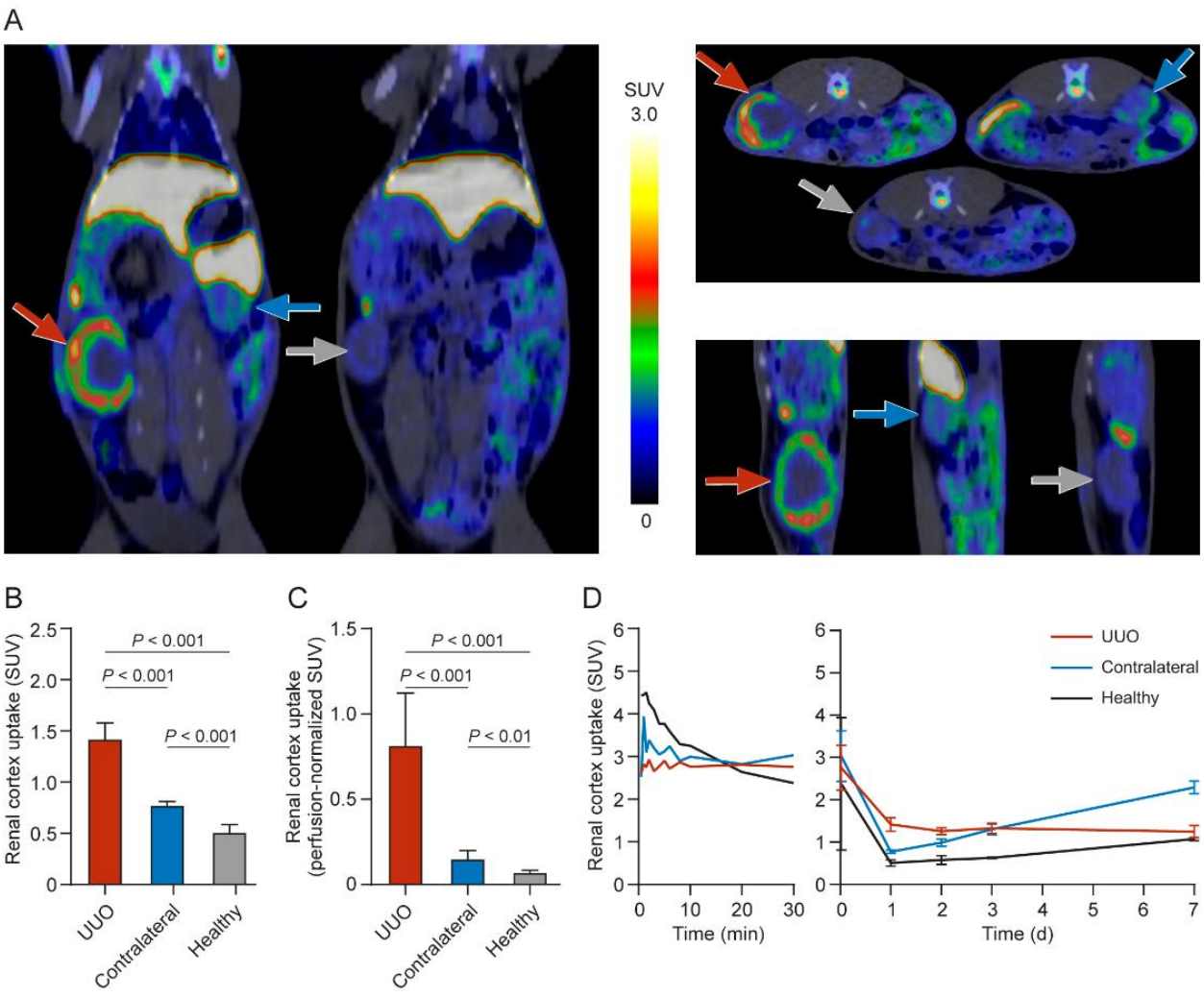

FIGURE 3. (A) Representative PET/CT images of two rabbits 24 hours after a single intravenous injection of ^{89}Zr-DFO-bexmarilimab. The red arrows denote UUO kidneys, the blue arrows show contralateral kidneys, and gray arrow denotes healthy kidneys. The radioactivity concentration in the renal cortex (B) without perfusion correction and (C) with ^{15}O-radiowater-based perfusion correction. (D) Time–activity curves of ^{89}Zr-DFO-bexmarilimab uptake in renal cortex.

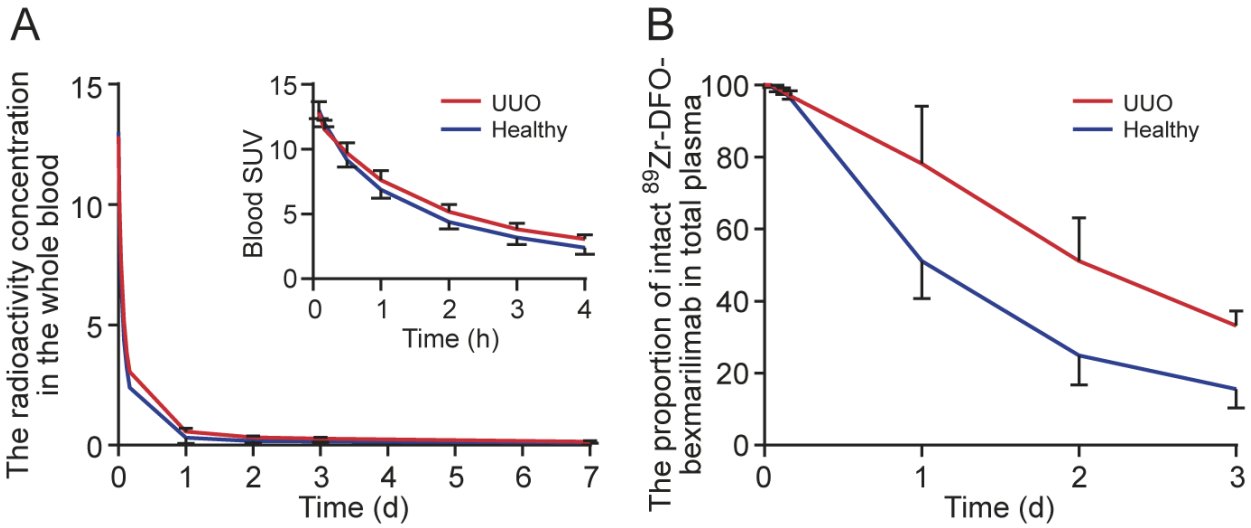

FIGURE 4. The distribution of ^{89}Zr-DFO-bexmarilimab in the rabbit blood circulation. (A) The radioactivity concentration in the whole blood. (B) The proportion of intact ^{89}Zr-DFO-bexmarilimab in total plasma. Lines represent mean values and bars are SDs of *n*=3 experiments.

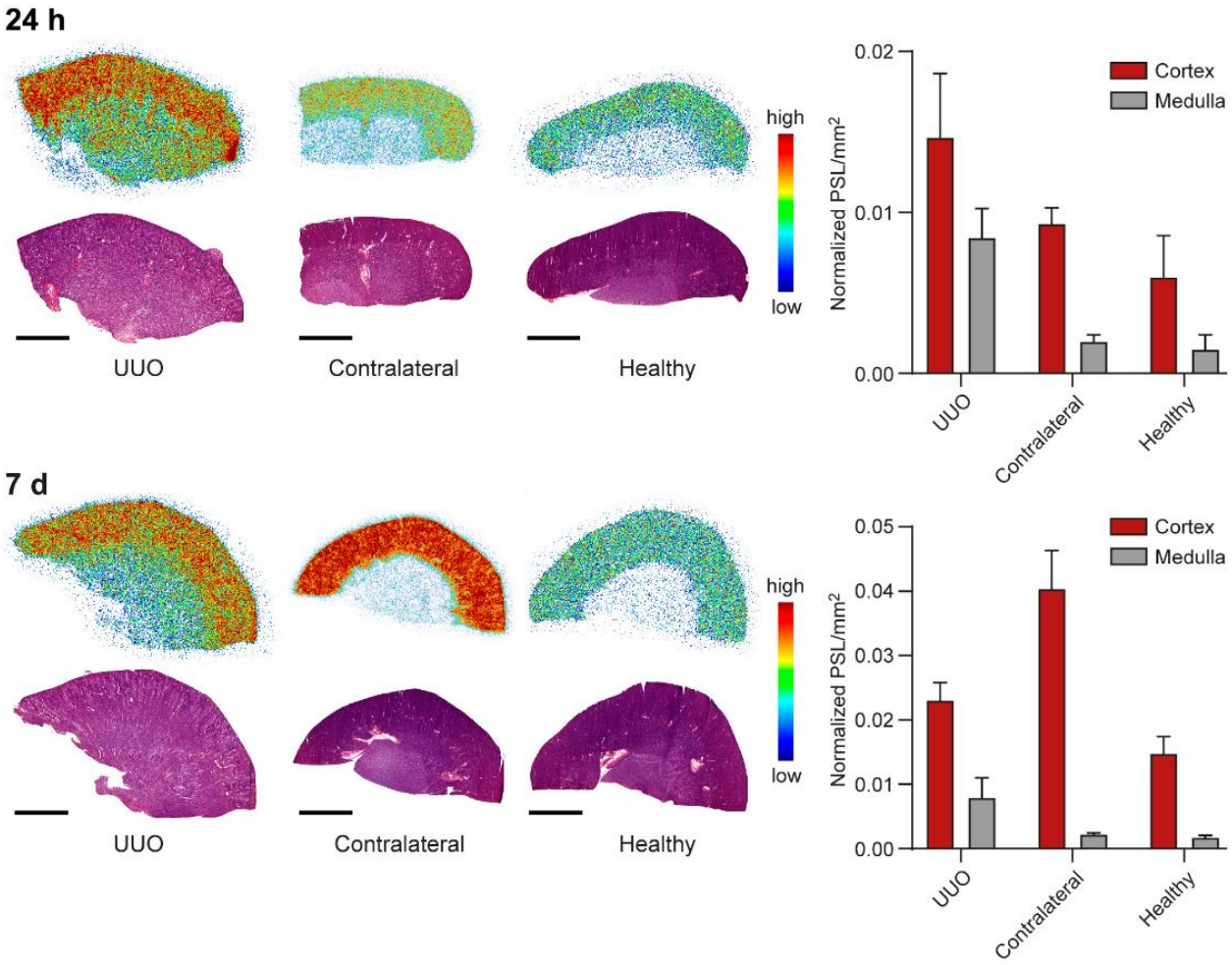

FIGURE 5. Representative *ex-vivo* digital autoradiographs and H&E staining of 20 µm kidney cryosections and quantification data 24 hours and 7 days after ^{89}Zr-DFO-bexmarilimab injection. The scale bar is 5 mm.

SUPPLEMENTAL MATERIAL

SUPPLEMENTAL MATERIALS AND METHODS

Rabbit UUO Model

Adult female New Zealand White rabbits were purchased from Lidköpings Kaninfarm (Sweden), Charles River Laboratories (France) or Envigo (UK) at 1.5–2.0 kg body weight. They were acclimatized for at least 12 days before entering the study. The rabbits received 125 g/day Rabma pelleted chow (Special Diets Service) 125 g/day, dried autoclaved hay twice a week, and tap water *ad libitum.*

Rabbits received 0.02 mg/kg buprenorphine (Temgesic 0.3 mg/mL; RB Pharmaceuticals) subcutaneously (s.c.) 30 minutes before the surgery. Anesthesia was initiated with s.c. injections of 2 mg/kg ketamine (Ketaminol 50 mg/kg Intervet Oy) mixed with 0.1 mg/kg medetomidine (Cepetor Vet 1 mg/mL; CP-Pharma) and 0.1 mg/kg midazolam (Midazolam Hameln 5 mg/mL, Hameln). A 22-gauge butterfly cannula was inserted into the marginal ear vein to allow for propofol (10 mg/kg) injection if needed. Maintenance of anesthesia was performed using 1–2% isoflurane by inhalation with oxygen (1 L/min).

The operation area was shaved, surgically cleaned and treated with lidocaine s.c. before incision. A lateral paramedian laparotomy was performed to allow the left ureter to be located, which was tied off with a non-absorbable suture to produce total obstruction. The laparotomy was closed by closing the abdominal muscle layer followed by the closure of the wound. After surgery, animals were returned to the pen once ambulatory. Rabbits were dosed with enrofloxacin antibiotic (Baytril 50 mg/mL; Bayer) 5 mg/kg s.c. and buprenorphine 0.02 mg/kg s.c. twice a day for 3 days post-surgery to provide analgesia.

A subset of rabbits (7 days after UUO operation [n = 5] and non-operated healthy control rabbits [n = 4]) were used for hematology and clinical chemistry analyses. Blood samples were drawn from the ear vein using a 21-gauge needle. Whole blood samples for hematology (Microvette 100 K3E EDTA tubes, Sarstedt & Co) and clinical chemistry (lithium-heparin coated Microvette 100 LH, Sarstedt & Co) were collected and analyzed using a VetScan HM5 hematology analyzer and a VetScan VS2 analyzer (Abaxis), respectively.

Radiosynthesis of ^{15}O-Radiowater

To obtain ^{15}O-H_2O, ^{15}O-O_2 was produced from ^{14}N-N_2 with a nuclear reaction $^{14}N(d, n)^{15}O$ and transformed into gaseous ^{15}O-H_2O on a Pt-catalyst at 700 ^{o}C in the presence of H_2. The gaseous ^{15}O-H_2O was directed into a radiowater generator (Hidex) that was installed adjacent to the PET/CT system to enable the formulation of ^{15}O-H_2O in saline and dosing to study subjects.

PET/CT Imaging

CT was performed before PET using technical parameters as follows: scan mode “helical”, helical slice thickness 3.75 mm; detector coverage 20 mm, pitch factor 1.375:1, voltage 100 kVp, current 10–80 mA, noise index 30, rotation time 0.8 sec, scan field of view (FOV) “large body”; display FOV 50.

PET images were reconstructed with an ordered subset expectation maximization algorithm and CT images were reconstructed using a soft tissue algorithm. Scatter correction, random counts, and dead-time corrections were all incorporated into the reconstruction algorithms. CT data were used for attenuation correction and were fused with PET images for anatomical reference.

Co-registration of PET and CT images was automatic and confirmed visually based on anatomical landmarks.

Plasma Pharmacokinetics

Plasma pharmacokinetic parameters, i.e., initial distribution volume (V_i), and total clearance (Cl_T) were calculated with in-house software using the blood radioactivity concentrations, and the function of intact ^{89}Zr-DFO-bexmarilimab in plasma over time after injection was used to calculate pharmacokinetic parameters. Calculation of these parameters was based on the radioactivity concentration at time zero (C_0) and the area under the curve from time zero to infinity ($AUC_{0-\infty}$), which were estimated by fitting a three-term exponential function f(x)=p1*e^(p2)+p3*e^(p4)+p5*e^(p6) to blood radioactivity concentration curves. V_i was calculated as Dose/C_0. Cl_T was calculated as Dose/AUC.

Residence Times and Radiation Dose Estimates

Absorbed doses, organ equivalent doses and effective doses were calculated with Organ Level INternal Dose Assessment/EXponential Modeling (OLINDA/EXM) software 2.2, which applies the RADAR method (developed by the RAdiation Dose Assessment Resource Task Group of the Society of Nuclear Medicine) for radiation dose calculations in internal exposure (1). The software includes radionuclide information and allows the selection of human body phantoms.

The residence times derived from rabbit data were integrated as the area under the TAC. The residence times were converted into corresponding human values by multiplication with a factor to scale organ and body weights: $(W_{TB,rabbit}/W_{Organ,rabbit}) \times (W_{Organ,human}/W_{TB,human})$, where $W_{TB,rabbit}$

and $W_{TB,human}$ are the total body weights of rabbit and human (70 kg), respectively; and $W_{Organ,rabbit}$ and $W_{Organ,human}$ are the organ weights of rabbit and human, respectively.

SUPPLEMENTAL RESULTS

Characterization of the UUO Rabbit Model

Analysis of kidney function parameters, namely blood urea nitrogen (BUN) and creatinine (CRE), at 7 days post-operation demonstrated that kidney function was not significantly disturbed. This finding indicates that the contralateral kidney compensates for the function of the UOO kidney. The BUN value of healthy control rabbits was 3.7 ± 0.4 mmol/L. On day 7 after the UUO surgery, BUN values had increased to 5.7 ± 0.5 mmol/L but remained within the reference range (3.6–11.4 mmol/L) for rabbits. The CRE values were 115.3 ± 43.8 μmol/L in healthy control rabbits and 96.4 ± 0.1 μmol/L on day 7 after the UUO surgery. Similarly, CRE values remained within the reference range (44–141 μmol/L) for rabbits. Additionally, analysis of hematological parameters remained within the reference range for rabbits (data not shown). Together, these findings suggest that the UUO disease model does not cause obvious clinical abnormalities. Importantly, post-operative recovery of the UUO-operated rabbits was uneventful; the animals were typically active and feeding within 12–24 hours and wounds healed within 4–5 days.

SUPPLEMENTAL REFERENCES

1. Stabin MG, Siegel JA. RADAR Dose Estimate Report: A Compendium of Radiopharmaceutical Dose Estimates Based on OLINDA/EXM Version 2.0. *J Nucl Med*. 2018;59:154–160.

SUPPLEMENTAL TABLE 1

Renal Perfusion ($mL_{blood}/mL_{tissue} \times min$) Determined Using ^{15}O-radiowater PET/CT

	UUO ($n = 6$)	Contralateral ($n = 6$)	Healthy ($n = 5$)	*P* values
Whole kidney	1.27 ± 0.56	4.25 ± 1.49	5.25 ± 0.55	0.001*; <0.001‡; 0.192‡
Cortex	2.00 ± 0.95	5.57 ± 1.96	7.19 ± 0.76	0.003*; <0.001‡; 0.116‡
Medulla	0.11 ± 0.03	0.58 ± 0.15	1.13 ± 0.23	<0.001*; <0.001‡; 0.001‡

Results are expressed as the mean ± SD. *P* values are from the independent samples t-test.

*UUO versus contralateral; ‡UUO versus healthy; ‡contralateral versus healthy.

SUPPLEMENTAL TABLE 2

Ex-Vivo Biodistribution of ^{89}Zr-DFO-Bexmarilimab in Rabbits

	24 hours after injection			7 days after injection		
	UUO rabbits (n = 4)	Healthy rabbits (n = 3)	P value	UUO rabbits (n = 3)	Healthy rabbits (n = 3)	P value
Kidney, UUO	1.93 ± 0.05	ND	<0.001*	2.24 ± 0.26	ND	0.010*
Kidney, contralateral	1.01 ± 0.05	ND	<0.001†	3.62 ± 0.27	ND	0.007†
Kidney, healthy	ND	1.00 ± 0.11	0.819‡	ND	1.39 ± 0.02	<0.001‡
Adrenal gland	1.78 ± 0.63	1.15 ± 0.09	0.206	1.39 ± 0.10	1.45 ± 0.29	0.809
Blood	0.47 ± 0.08	0.31 ± 0.01	0.029	0.14 ± 0.05	0.27 ± 0.22	0.463
Bone (femur)	0.40 ± 0.08	0.40 ± 0.13	0.992	0.81 ± 0.11	0.55 ± 0.08	0.062
Bone marrow	1.51 ± 0.10	1.09 ± 0.14	0.011	2.39 ± 0.18	1.52 ± 0.34	0.034
Brain	0.02 ± 0.00	0.02 ± 0.00	0.162	0.02 ± 0.00	0.01 ± 0.00	0.182
Cecum (with contents)	0.98 ± 0.06	1.06 ± 0.17	0.487	0.13 ± 0.09	0.04 ± 0.03	0.212
Feces	1.19 ± 0.22	1.15 ± 0.19	0.844	0.10 ± 0.10	0.02 ± 0.00	0.298
Gall bladder	1.96 ± 0.90	3.14 ± 0.95	0.216	1.50 ± 0.66	1.27 ± 0.59	0.725
Heart	0.41 ± 0.06	0.20 ± 0.16	0.096	0.25 ± 0.03	0.26 ± 0.02	0.868
Large intestine, lower	0.10 ± 0.11	0.15 ± 0.01	0.577	0.17 ± 0.02	0.14 ± 0.01	0.089
Large intestine, upper	0.24 ± 0.03	0.20 ± 0.04	0.307	0.18 ± 0.01	0.14 ± 0.00	0.003
Liver	24.22 ± 2.28	22.91 ± 2.02	0.535	19.51 ± 1.81	22.38 ± 0.70	0.104
Lungs	0.42 ± 0.07	0.26 ± 0.16	0.193	0.32 ± 0.07	0.27 ± 0.02	0.379
Lymph node	0.92 ± 0.17	0.65 ± 0.30	0.250	0.71 ± 0.12	0.45 ± 0.10	0.079
Muscle	0.03 ± 0.00	0.03 ± 0.01	0.383	0.02 ± 0.00	0.02 ± 0.00	0.993
Ovary	1.01 ± 0.07	0.53 ± 0.19	0.013	0.67 ± 0.12	0.57 ± 0.06	0.395
Pancreas	0.17 ± 0.02	0.17 ± 0.06	0.904	0.19 ± 0.03	0.19 ± 0.06	0.957
Salivary gland	0.24 ± 0.05	0.20 ± 0.06	0.497	0.20 ± 0.03	0.15 ± 0.02	0.130
Skin	0.12 ± 0.02	0.12 ± 0.03	0.869	0.05 ± 0.02	0.05 ± 0.01	0.578
Small intestine	0.69 ± 0.32	0.34 ± 0.23	0.229	0.09 ± 0.02	0.04 ± 0.03	0.096
Spleen	6.10 ± 0.59	4.26 ± 1.53	0.124	7.42 ± 1.62	3.81 ± 0.16	0.035
Stomach (with contents)	0.62 ± 0.33	0.54 ± 0.23	0.767	0.07 ± 0.01	0.03 ± 0.03	0.174
Thymus	0.12 ± 0.01	0.20 ± 0.13	0.325	0.17 ± 0.04	0.08 ± 0.00	0.022
Thyroid gland	0.12 ± 0.01	0.32 ± 0.24	0.227	0.15 ± 0.03	0.12 ± 0.04	0.432
Urinary bladder	0.43 ± 0.05	0.41 ± 0.06	0.656	0.26 ± 0.04	0.37 ± 0.14	0.355
Urine	0.42 ± 0.12	0.16 ± 0.17	0.246	0.16 ± 0.06	0.09 ± 0.04	0.240
Uterus	0.59 ± 0.06	0.45 ± 0.03	0.026	0.32 ± 0.07	0.18 ± 0.01	0.049
White adipose tissue	0.13 ± 0.05	0.05 ± 0.01	0.065	0.09 ± 0.02	0.04 ± 0.00	0.035

Results are expressed as standardized uptake values, mean ± SD. UUO, unilateral ureteral obstruction. ND, not determined. P values are from the independent samples t-test. *UUO kidney versus healthy kidney; †UUO kidney versus contralateral kidney; ‡UUO contralateral kidney versus healthy kidney.

SUPPLEMENTAL TABLE 3

Plasma Pharmacokinetic Parameters of ^{89}Zr-DFO-Bexmarilimab in Rabbits

Parameter	Total radioactivity			Intact ^{89}Zr-DFO-bexmarilimab		
	UUO (n = 3)	Healthy (n = 3)	P value	UUO (n = 3)	Healthy (n = 3)	P value
AUC (h*kBq/mL)	940.9 ± 182.7	578.0 ± 74.3	0.060	465.3 ± 57.6	279.7 ± 2.5	0.010
Cl_T (mL/h)	10.4 ± 2.1	17.4 ± 2.1	0.030	20.4 ± 1.5	35.4 ± 1.0	<0.001
C_0 (kBq/mL)	117.0 ± 11.8	112.1 ± 19.8	0.779	113.1 ± 19.3	113.1 ± 19.3	0.763
Vi (mL)	80.9 ± 3.5	91.0 ± 16.0	0.431	80.0 ± 2.8	90.1 ± 15.4	0.416

AUC, area under curve; Cl_T, total clearance; C_0, initial concentration; Vi, initial distribution volume

SUPPLEMENTAL TABLE 4

Normalized Number of Disintegrations in Source Organs for ^{89}Zr-DFO-Bexmarilimab Extrapolated from Healthy Rabbit Data

Organ	Disintegrations (hours)
Bone	3.565 ± 0.918
Bone marrow	6.519 ± 2.078
Heart wall	0.471 ± 0.042
Kidney	0.355 ± 0.045
Liver	62.065 ± 12.186
Muscle	1.309 ± 0.664
Spleen	0.676 ± 0.462

Results are expressed as the mean ± SD (n = 3).

SUPPLEMENTAL TABLE 5

Human Radiation Dose Estimates for ^{89}Zr-DFO-Bexmarilimab Extrapolated from Healthy Rabbit Data

Organ	Dose (mGy/MBq)
Adrenal glands	1.777 ± 0.240
Brain	0.179 ± 0.038
Esophagus	0.754 ± 0.065
Eyes	0.182 ± 0.038
Gallbladder wall	2.580 ± 0.420
Left colon	0.494 ± 0.017
Small intestine	0.491 ± 0.014
Stomach wall	0.714 ± 0.044
Right colon	0.832 ± 0.061
Rectum	0.298 ± 0.053
Heart wall	0.939 ± 0.099
Kidneys	0.996 ± 0.102
Liver	5.860 ± 1.100
Lungs	0.661 ± 0.047
Pancreas	0.930 ± 0.074
Prostate	0.297 ± 0.041
Salivary glands	0.220 ± 0.043
Red marrow	0.646 ± 0.076
Osteogenic cells	0.556 ± 0.087
Spleen	0.833 ± 0.318
Testes	0.187 ± 0.041
Thymus	0.438 ± 0.001
Thyroid	0.297 ± 0.027
Urinary bladder wall	0.264 ± 0.048
Total body	0.357 ± 0.019
Effective dose	0.702 ± 0.051*

Results are expressed as the mean ± SD (n = 3). *mSv/MBq

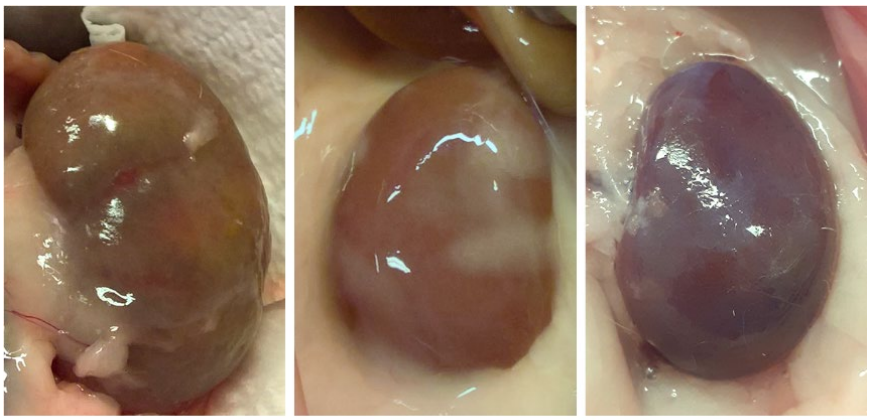

SUPPLEMENTAL FIGURE 1. Photographs of representative rabbit kidneys 14 days after UUO surgery.

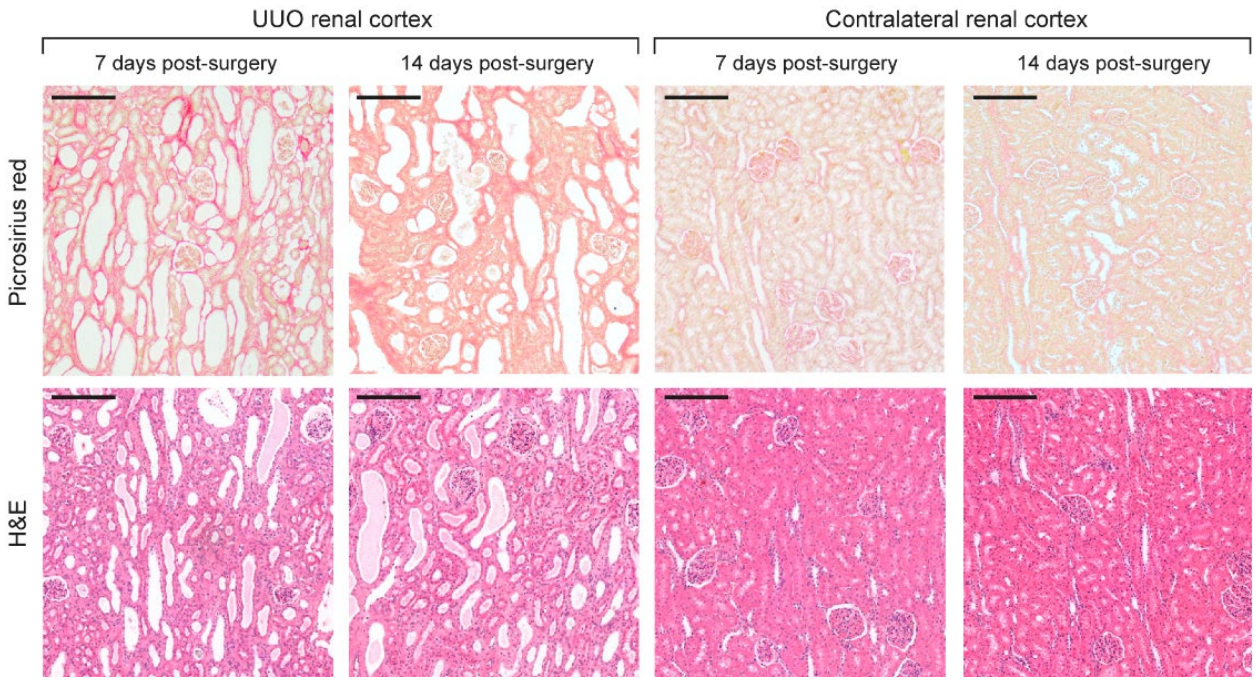

SUPPLEMENTAL FIGURE 2. Representative Picrosirius red and H&E staining of rabbit renal cortex at 7 and 14 days after unilateral ureteric obstruction (UUO) surgery. The scale bar is 200 μm.

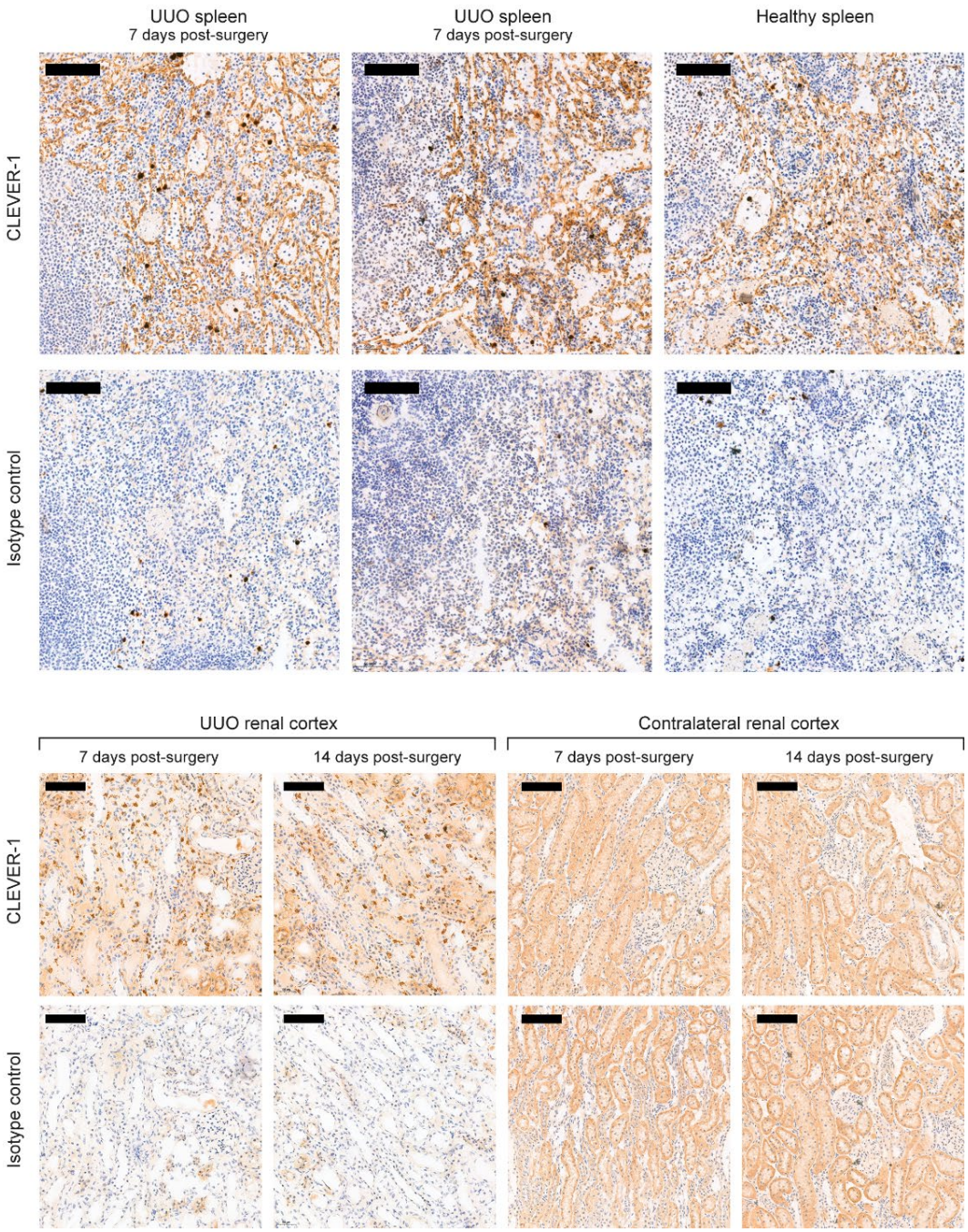

SUPPLEMENTAL FIGURE 3. Representative CLEVER-1 immunohistochemical staining of rabbit spleen and renal cortex 7 and 14 days after UUO surgery and in a healthy rabbit. There was no detectable difference in CLEVER-1 expression tissues collected at 7 and 14 days after surgery. The scale bar is 100 μm.

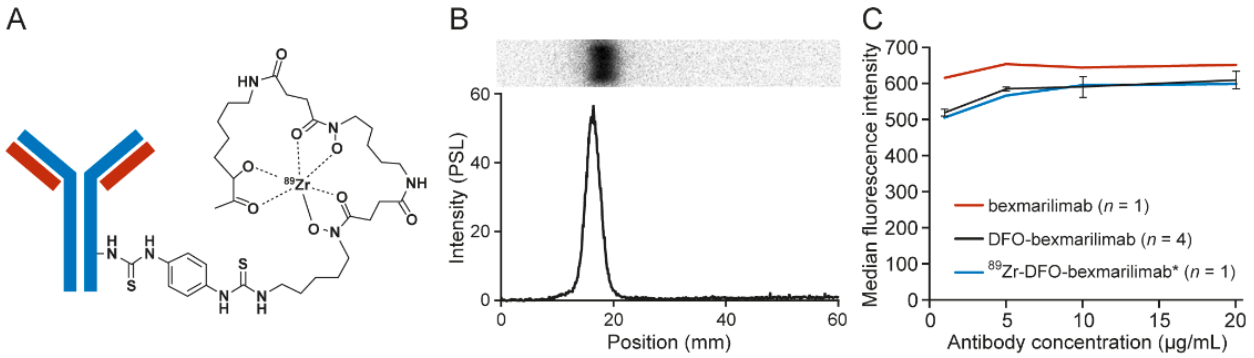

SUPPLEMENTAL FIGURE 4. Preparation of ^{89}Zr-DFO-bexmarilimab and immunoreactivity. (A) The molecular structure of ^{89}Zr-labeled desferrioxamine (DFO)-conjugated bexmarilimab. (B) Representative quality control analysis of ^{89}Zr-DFO-bexmarilimab based on sodium dodecyl sulfate-polyacrylamide gel electrophoresis (SDS-PAGE). Upper panel, a digital autoradiograph of the SDS-PAGE analysis. Lower panel, the chromatogram of the lane. PSL, photostimulated luminescence. (C) The effect of DFO-conjugation and ^{89}Zr-labeling on the binding of bexmarilimab to CLEVER-1. *Measured after radioactive decay.

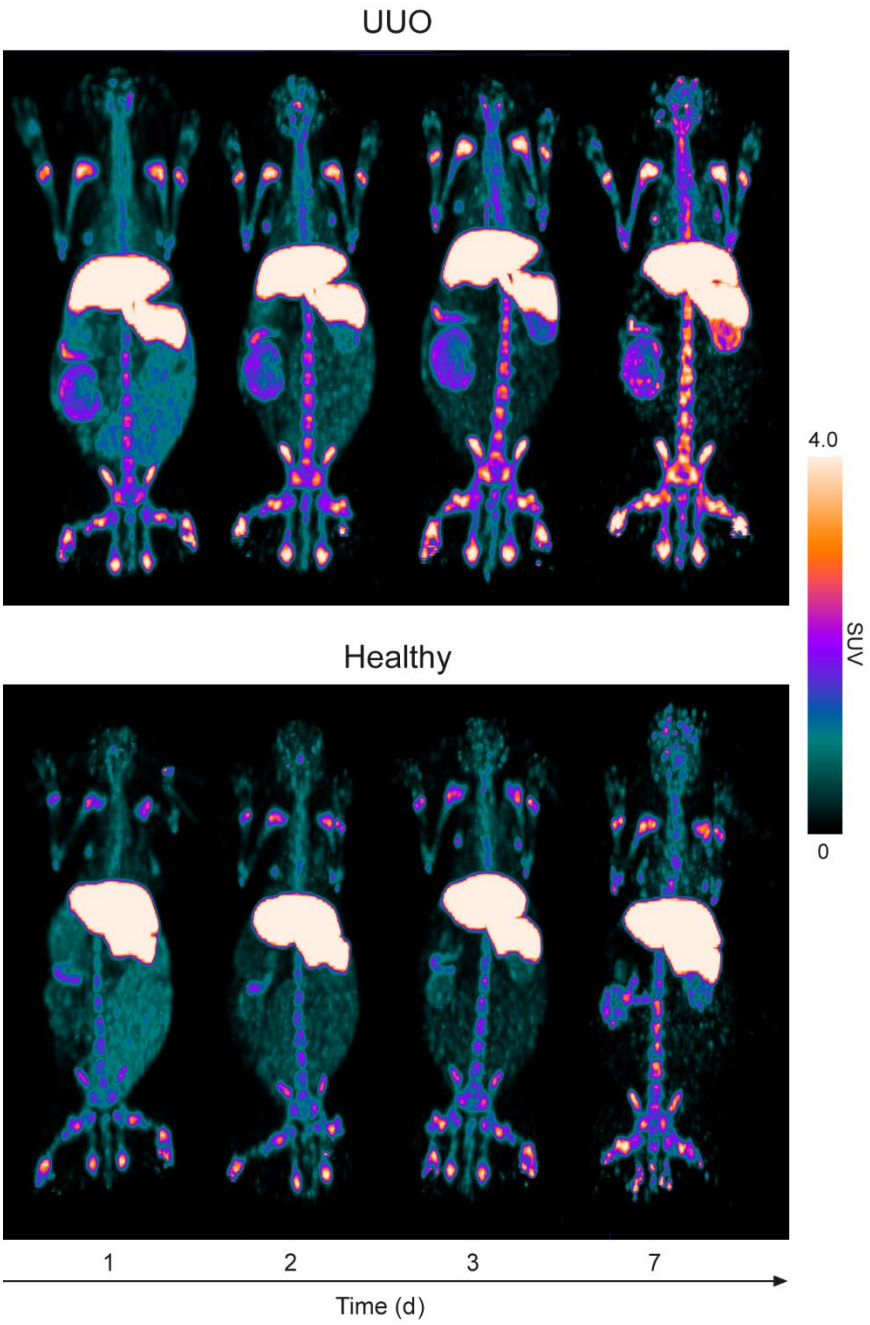

SUPPLEMENTAL FIGURE 5. Sequential maximum intensity projection PET images of UUO-operated and healthy rabbits.

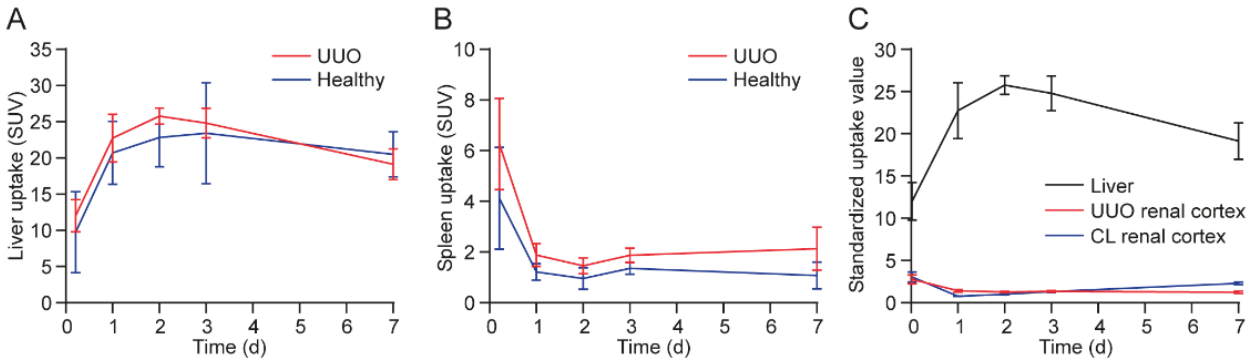

SUPPLEMENTAL FIGURE 6. Time–activity curves of ^{89}Zr-DFO-bexmarilimab uptake in rabbit (A) liver, (B) spleen, and (C) the liver versus UUO renal cortex and the contralateral (CL) renal cortex.

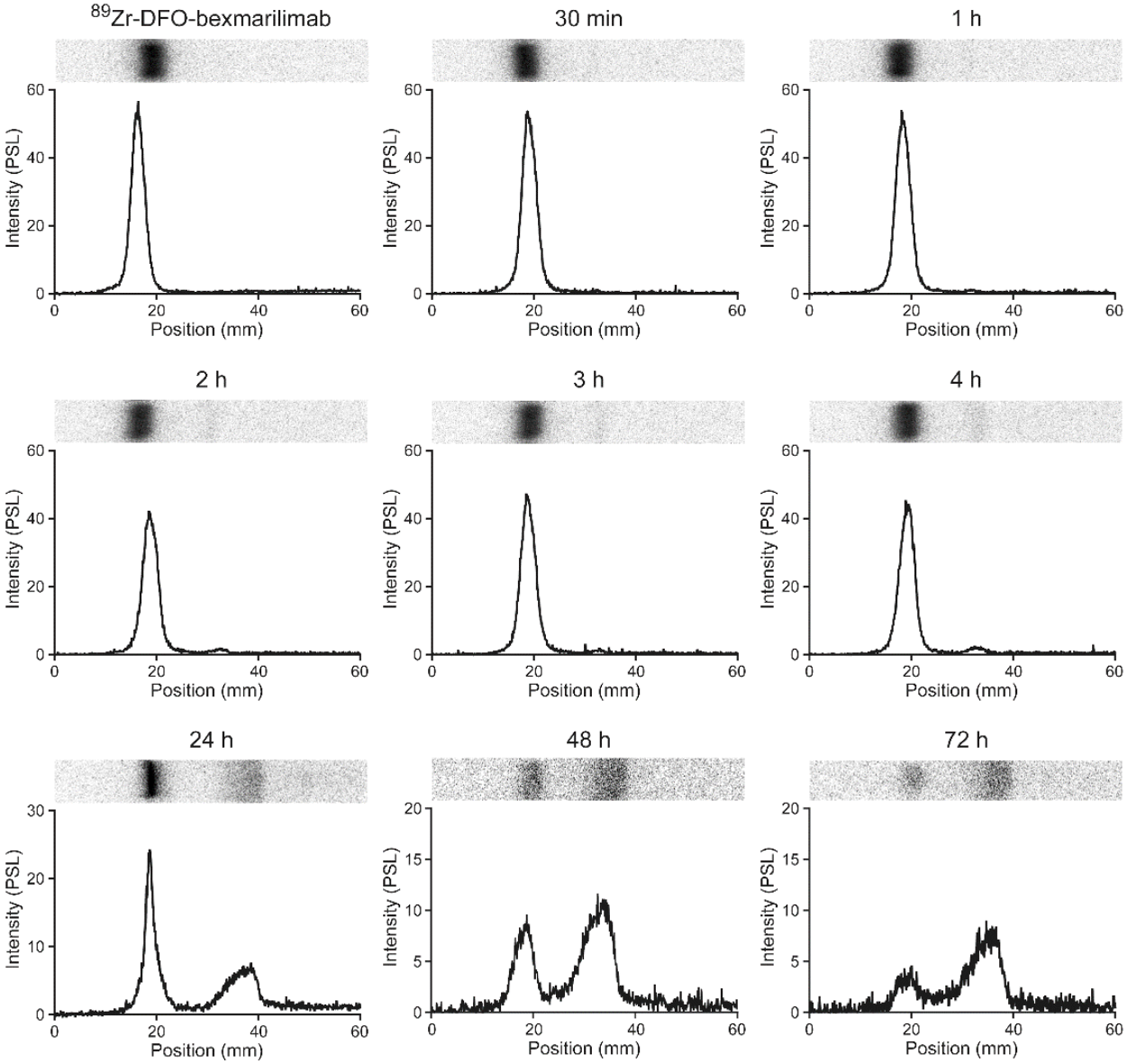

SUPPLEMENTAL FIGURE 7. Representative SDS-PAGE autoradiographs of ^{89}Zr-DFO-bexmarilimab in rabbit plasma at different time points after injection.

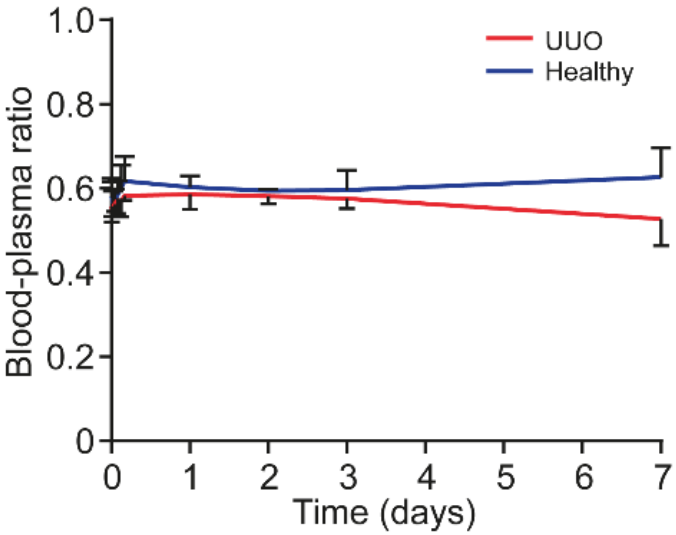

SUPPLEMENTAL FIGURE 8. The blood-plasma ratio of radioactivity. The lines represent the mean values and bars are standard deviations of $n = 3$ experiments.

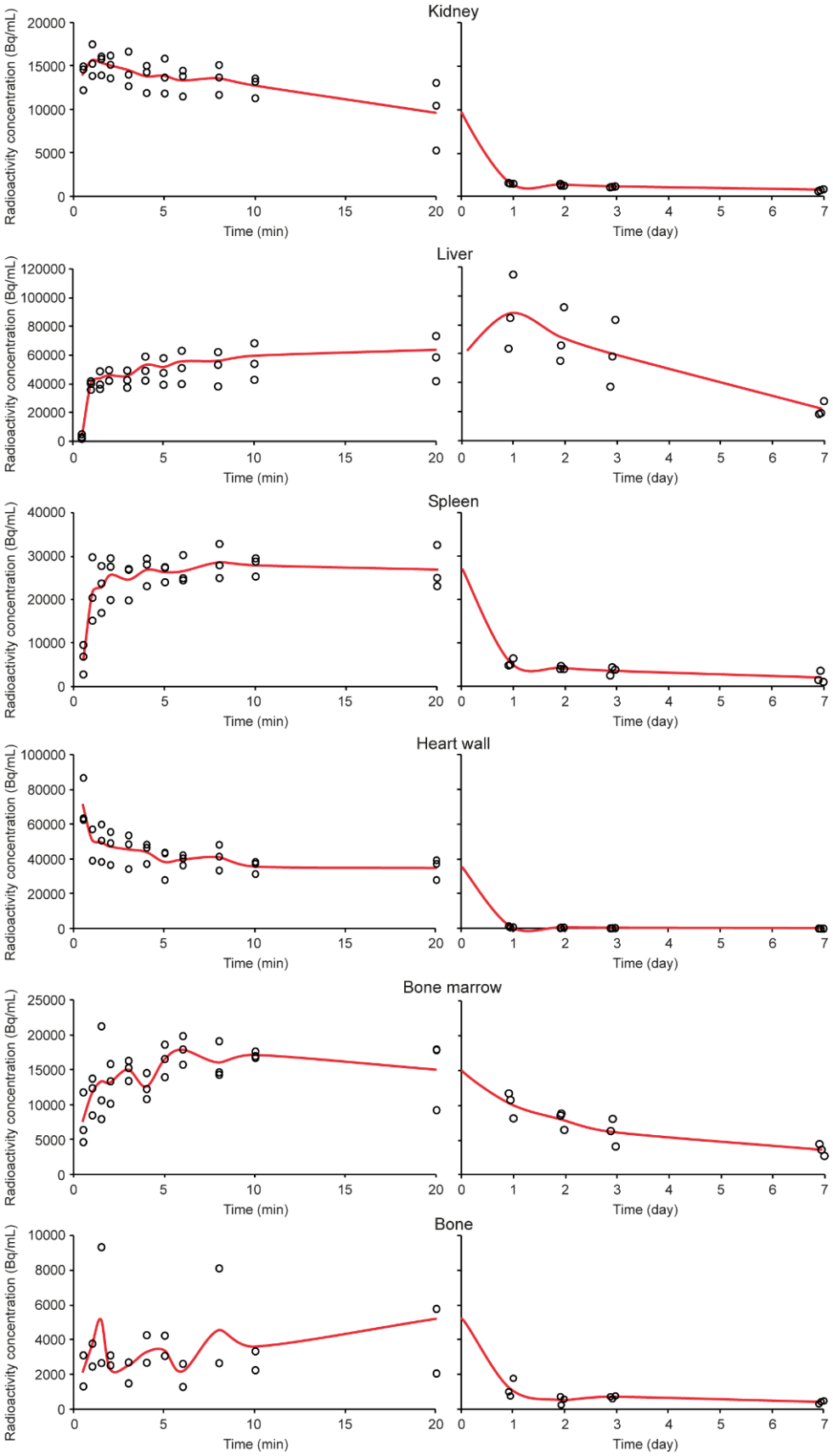
Kidney
Liver
Spleen
Heart wall
Bone marrow
Bone
Radioactivity concentration (Bq/mL)
Time (min)
Time (day)

SUPPLEMENTAL FIGURE 9. Radioactivity concentration (non-decay-corrected) in healthy rabbit tissues as a function of time after intravenous injection of ^{89}Zr-DFO-bexmarilimab; the radioactivity concentrations were used to estimate the human radiation doses. The red lines show the mean and the open circles are the measured values.